Journal of Alloys and Compounds 509 (2011) 6077–6082

Contents lists available at ScienceDirect

Journal of Alloys and Compounds

journal homepage: www.elsevier.com/locate/jallcom

Influence of La doping on elastic and thermodynamic properties of $SrMoO_3$

Nupinderjeet Kaur[a], Rajneesh Mohan[b,*], N.K. Gaur[c], R.K. Singh[d]

[a] Department of Physics, Regional Institute of Education, Bhopal 462013, India
[b] Mechatronics, Jeju National University, Jeju 690-756, Republic of Korea
[c] Department of Physics, Barkatullah University, Bhopal 462026, India
[d] School of Basic Sciences, ITM University, Gurgaon 122 017, India

ARTICLE INFO

Article history:
Received 7 May 2010
Received in revised form 3 March 2011
Accepted 4 March 2011
Available online 12 March 2011

PACS:
74.25.Kc
61.50.Lt
72.80.Ga
65.40.Ba
74.25.Bt

Keywords:
Elastic properties
Cohesive properties
Specific heat
Molybdate
Thermodynamic properties

ABSTRACT

The elastic and thermodynamic properties for $Sr_{1-x}La_xMoO_3$ (x = 0.0, 0.05, 0.1, 0.15, and 0.2) with temperature have been investigated, probably for the first time, by using modified rigid ion model (MRIM). The computed results on the elastic constants (C_{11}, C_{12}, and C_{44}) are the first report on them. Using these elastic constants we have computed other elastic properties such as B, β, G', G, E, σ, B/G ratio, Cauchy pressure ($C_{12} - C_{44}$) and Lame's parameters (μ, λ). We have also reported the thermodynamic properties such as ϕ, f, θ_D, θ_{D1}, υ_0, υ_1, γ, and α. The values of Young's modulus, shear modulus and compressibility for $SrMoO_3$ are in good agreement with the available experimental data. The concentration (x) dependence of θ_D in $Sr_{1-x}La_xMoO_3$ suggests that increased La doping drives the system effectively away from the strong electron–phonon coupling regime. Specific heat is reported in the wide temperature range and compared with the respective experimental data available in the literature. The thermal expansion coefficient of $SrMoO_3$ is in good agreement with the other theoretical data.

1. Introduction

Transition-metal oxides (TMOs) have attracted a lot of attention for a long time because of their importance in both the fundamental aspects of condensed-matter physics and the potential for technological applications. The $A_{n+1}B_nO_{3n+1}$-type perovskite 3d TMO attracted considerable attention due to the discovery of high-temperature superconductivity (SC) in cuprates [1] and colossal magnetoresistance (CMR) [2] in manganites.

With the passage of time, the scope of research has broadened to include 4d/5d TMOs from 3d TMOs. The central characteristic of these 4d and 5d shell-based TMOs is more extended d orbitals of transition-metal ions as compared to those of 3d-shell ions [3]. It has been generally believed that the electrons in these orbitals feel rather weak on-site Coulomb repulsion energy and the 4d orbitals hybridize more strongly with their neighbouring orbits, e.g., O 2p orbitals, than the 3d orbitals. As a result, the physical properties of these 4d or 5d TMOs are sensitive to perturbations, such as magnetic fields, pressure or chemical doping.

$SrMoO_3$, a 4d TMO has been widely studied due to its interesting physical properties in the past few years. It is a cubic perovskite showing Pauli paramagnetism, and metallic conductivity [4–6]. The metallic conductivity of $SrMoO_3$ is related to the $4d^2$ delocalized electrons of Mo^{4+} cations which act as carriers in the material [7], its high conductivity and low raw-material costs are attractive for practical applications [8]. And the charge-transfer energy ($\Delta_{pd} \sim 5$ eV) of $SrMoO_3$ is so large that it can be classified as a possible superconducting material according to the criterion established by Goodenough [9] and [10]. However, no observation of a superconducting transition has been observed down to 36 mK in $SrMoO_3$ single crystal due to the extremely small electron–phonon interaction [7].

Zhang et al. have done a systematic study of many pure and doped perovskite molybdate oxides such as $SrMo_{1-x}B_xO_3$ (B = Mn, Cu, Cr) [11–13] and $Sr_{1-x}A_xMoO_3$ (A = La and Pr) [14,15] on the structural, electronic transport and magnetic properties. Agarwal et al. [4] have done calorimetric investigations of $SrMoO_3$ and $BaMoO_3$ compounds. Lee et al. reported the systematic inves-

* Corresponding author: Tel.: +82 64 7543715; fax: +82 64 7563886.
E-mail address: rajneesh482@gmail.com (R. Mohan).

0925-8388/$ – see front matter © 2011 Elsevier B.V. All rights reserved.
doi:10.1016/j.jallcom.2011.03.025

tigations on the thermal, electrical, and mechanical properties of barium and strontium series perovskite-type oxides, such as Ba(Zr,Ce)O_3 [16,17], $BaMoO_3$ [18], Sr(Hf,Ru)O_3 [19] and 4d $SrMO_3$ (M = Zr, Mo, Ru, and Rh) [3] using optical conductivity analyses. Structural and magnetic properties of $SrFe_xMo_{1-x}O_3$ were reported by Kawachi et al. [20]. Recently Macquart et al. [21] studied phase transition in SrMoO3 using neutron diffraction. Logvinovicha et al. [22] have reported the synthesis procedure for higher level substituted oxynitrides of the composition $SrMoO_{3-x}N_x$ and characterised them for crystallographic structure and physical properties by neutron diffraction (ND) XRD, X-ray absorption near edge spectroscopy, Seebeck coefficient and electrical conductivity measurements. But no efforts have been made to study the elastic properties of these molybdates. Therefore, in this paper, probably for the first time, we have made an attempt to carry out systematic study the elastic and thermodynamic properties of $SrMoO_3$ and the effect of La substitution on these properties by using modified rigid ion model (MRIM).

Recently, we have successfully shown the thermodynamic behaviour of manganites [23–27] and diborides [28,29], by using MRIM. The major contribution to the pair potential of MRIM is of the long-range (LR) Coulomb attraction, which is counterbalanced by the short-range (SR) overlap repulsion having their origin in the Pauli exclusion principle. This SR interaction is expressed by a Hafemeister–Flygare (HF) [30] type overlap repulsion effective up to the second neighbour ions. This potential also incorporates the effects of the van der Waals (vdW) attraction (Tosi and Fumi [31]) arising from the dipole–dipole (d–d) and dipole–quadrupole (d–q) interactions, whose coefficients are estimated from the Slater–Kirkwood variational (SKV) [32] approach, which treats both the ions (cations and anions) as polarizable. Motivated from such a realistic and qualitative representation of the interionic potential and its versatile applicability to describe the cohesive and physical properties of solids and alloys (Singh [33] and Varshney et al. [34]), we thought it is pertinent to apply this MRIM, probably for the first time, to explore the elastic and thermodynamic properties of the pure and doped $SrMoO_3$. The interaction potential of the MRIM is described in Section 2. The computed results are presented and discussed in Section 3.

2. Theoretical methods

2.1. Modified rigid ion model (MRIM)

The interionic potential of the rigid ion model (RIM) [29,33] is formulated on the basis of the simple Born model, according to which the ions are treated as the rigid (or unpolarisable) ions held together in crystals by the long-range (LR) Coulomb attraction and prevented from the collapsing by the short-range (SR) overlap repulsion. This potential was modified by Fumi and Tosi [31] by incorporating the effect of van der Waals (vdW) attraction due to the d–d and d–q interactions to reveal the cohesive properties of ionic solids. Also, the overlap repulsion was extended up to the second neighbour ions by Hafemeister and Flygare (HF) [30].

In the present investigation, we have modified the RIM potential by including the vdW attraction and HF type overlap repulsion to describe the elastic and thermodynamic properties of $Sr_{1-x}La_xMoO_3$ (x = 0.0, 0.05, 0.1, 0.15, and 0.2). The effective interionic potential corresponding to the MRIM framework is expressed as:

$$\phi = -\frac{e2}{2}\sum_{kk'} ZkZk'r - 1kk' - \sum_{kk'} ckk'r - 6kk' - \sum_{kk'} dkk'r - 8kk' + nb1\beta kk' \exp\left\{\frac{(r_k + r_{k'} - r_{kk'})}{\rho 1}\right\} + \frac{n'}{2}b2\left[\beta kk \exp\left\{\frac{2rk - rkk}{\rho 2}\right\} + \beta k'k' \exp\left\{\frac{2rk' - rk'k'}{\rho 2}\right\}\right] \quad (1)$$

Here, the first term represents the LR Coulomb energy. The second and third terms are the SR vdW energies due to d–d and d–q interactions, respectively. The last two terms are the SR repulsive energies due to the overlap repulsion between the nearest (kk') and the next nearest (nn) neighbour (kk and $k'k'$) ions, respectively. Z_k ($Z_{k'}$) and r_k ($r_{k'}$) are the ionic charges and radii of k (k') ions. Also, $r_{kk'}$ and r_{kk} (= $r_{k'k'}$) are the interionic separations between the nearest k(k') and the next nearest kk(=$k'k'$) neighbour ions. The symbols $c_{kk'}$ and $d_{kk'}$ represent the vdW coefficients due to d–d and d–q interactions, respectively. b_1 (ρ_1) and b_2 (ρ_2) are the range (hardness) parameters corresponding to the Sr/La–O and Mo–O bond distances for these $Sr_{1-x}La_xMoO_3$ compounds. $\beta_{kk'}$ [=1 + (Z_k/n_k) + ($Z_{k'}/n_{k'}$)] are the Pauling coefficients [35]. The vdW coefficients ($c_{kk'}$ and $d_{kk'}$) are evaluated from the Slater–Kirkwood variational (SKV) method [32].

The present interionic potential of MRIM contains two-model parameters b and ρ, which have been determined from the equilibrium condition,

$$\left(\frac{d\phi}{dr}\right)_{r=r_0} = 0 \quad (2)$$

and the bulk modulus,

$$B = (9Kr_0)^{-1}\left[\frac{d2\phi}{dr2}\right]_{r=r_0} \quad (3)$$

where K is the structure dependent constant. r_0 is the equilibrium interatomic separation. The model parameters b (ρ) when calculated corresponding to Sr/La–O and Mo–O bond distances then they effectively become four model parameters b_1 (ρ_1) and b_2 (ρ_2) for the $Sr_{1-x}La_xMoO_3$ compounds.

2.2. Elastic properties

Using Eq. (1), the expressions for second-order elastic constants (SOECs) [27,36] are expressed as:

$$C11 = 4.133T\beta BT + \frac{e2}{4r4}\left[\frac{A1}{6} - 1.7333B1 + \frac{A2}{2} - 2.0666B2\right] \quad (4)$$

$$C12 = 3.0666T\beta BT + \frac{e2}{4r4}\left[\frac{A1}{6} - 1.3666B1 + \frac{A2}{2} - 1.5333B2\right] \quad (5)$$

$$C44 = -2.0666T\beta BT + \frac{e2}{4r4}\left[\frac{A1}{6} - 1.3666B1 + \frac{A2}{2} - 1.5333B2\right] \quad (6)$$

$$T\beta BT = \frac{e2}{4r4}[0.3392\varepsilon 2 + B1 + B2] \quad (7)$$

where A_1, A_2, B_1 and B_2 are the short-range parameters [33], β is the volume thermal expansion coefficient and B_T is the isothermal bulk modulus. e is the electronic charge and $\in$ is the ionic charge.

For a cubic structure, the bulk modulus B and the shear modulus G are taken as:

$$B = \frac{C_{11} + 2C_{12}}{3} \quad (8)$$

$$G = \frac{3C_{44} + C_{11} - C_{12}}{5} \quad (9)$$

Also, the Young's modulus (E) and the Poisson's ratio (σ) are given by:

$$E = \frac{9BG}{3B + G} \quad (10)$$

$$\sigma = \frac{1}{2}\left(1 - \frac{E}{3B}\right) \quad (11)$$

Using Poisson's ratio σ the Lamé's coefficients (μ and λ), for $Sr_{1-x}La_xMoO_3$ have been obtained as:

$$\mu = \frac{E}{2(1+\sigma)} \quad (12)$$

$$\lambda = \frac{\sigma E}{(1+\sigma)(1-2\sigma)} \quad (13)$$

The shear and longitudinal sound velocities υ_s and υ_l are obtained from Navier's equation as follows [37]:

$$\upsilon s = \sqrt{\frac{G}{\rho}} \quad (14)$$

$$\upsilon l = \sqrt{\frac{B + (4/3)G}{\rho}} \quad (15)$$

The average sound velocity υ_m [38] is obtained from:

$$\upsilon_m = \left[\frac{1}{3}\left(\frac{2}{\upsilon_s^3} + \frac{1}{\upsilon_l^3}\right)\right] \quad (16)$$

where υ_s and υ_l are the shear and longitudinal sound velocities, respectively.

The Debye temperature may be estimated from the average sound velocity υ_m [38] as:

$$\theta D = \frac{h}{k}\left[\frac{3n}{4\pi}\left(\frac{NA\rho}{M}\right)\right]^{1/3}\upsilon m \quad (17)$$

where h is Planck's constants, k is Boltzmann's constant, N_A is Avogadro's number, n is the number of atoms per formula unit, M is the molecular mass per formula unit, and ρ is the density.

Table 1
Model parameters (b_1, ρ_1, b_2, and ρ_2) of $Sr_{1-x}La_xMoO_3$ (x = 0.0, 0.05, 0.1, 0.15, and 0.2).

Parameters	0.0	0.05	0.1	0.15	0.2
(Sr/La–O)					
b_1	23.51	22.93	22.82	22.78	22.73
ρ_1	0.537	0.489	0.488	0.487	0.476
(Mo–O)					
b_2	18.95	18.05	17.96	17.92	17.88
ρ_2	0.281	0.273	0.272	0.271	0.270

2.3. Thermodynamic properties

The lattice specific heat at constant volume can be calculated using the expression [24–26],

$$CV = \frac{12\pi 4NAk}{5}\left(\frac{T}{\theta D}\right)^3 \int_0^{\theta D/T} \frac{x4ex}{(ex-1)^2}dx \quad (18)$$

where N_A, k, θ_D has there usual meanings, defined above.

The lattice specific heat at constant pressure C_p can now be computed from the relation:

$$CP = CV + 9\alpha 2BTVT \quad (19)$$

where α, B_T, V, and T are the thermal expansion coefficient, isothermal bulk modulus, unit cell volume and temperature, respectively.

The value of thermal expansion coefficient (α) is obtained from the well known relation:

$$\alpha = \frac{\gamma CV}{BV} \quad (20)$$

where γ is the Gruneisen parameter, calculated from the relation:

$$\gamma = -\left(\frac{r0}{6}\right)\left[\frac{\phi'''(r)}{\phi''(r)}\right]_{r=r_0} \quad (21)$$

The Debye temperature (θ_D) from Eq. (17), gives us the Restrahalen frequency (υ_o) as,

$$\upsilon 0 = \frac{\theta Dk}{h} \quad (22)$$

where h and k have their usual meanings as defined above.

Restrahalen frequency (υ_1) calculated from the molecular force constant (f) as:

$$\upsilon_1 = \left(\frac{1}{2\pi}\right)\left[\frac{f}{\mu}\right]^{1/2} \quad (23)$$

where, μ is the reduced mass of the system and the molecular force constant is expressed as:

$$f = \frac{1}{3}\left[\phi''^R_{kk'}(r) + \frac{2}{r}\phi'^R_{kk'}\right]_{r=r_0} \quad (24)$$

where $\phi Rkk'(r)$ is the Hafemeister Flygare [30] type interactions defined in Eq. (1).

3. Results and discussion

3.1. Model parameters

The Model (MRIM) described above has been applied to the compounds with perovskite structure. Its applicability is first of all tested by computing the cohesive energy of $Sr_{1-x}La_xMoO_3$ (x = 0.0, 0.05, 0.1, 0.15, and 0.2) compounds using Eq. (1). We have obtained the model parameters as a function of temperature using the lattice parameters taken from Refs. [14,39] and the van der Waals coefficients are determined from SKV method [34] on the lines of our earlier paper [23–29]. Bulk modulus is computed by the heterogeneous-metal-mixture rule (HMMR) [40]. The values of these model parameters (b_1, ρ_1) and (b_2, ρ_2) for $Sr_{1-x}La_xMoO_3$ (x = 0.0, 0.05, 0.1, 0.15, and 0.2) perovskites are depicted in Table 1, respectively and used to describe various physical properties of the present system of pure and doped $SrMoO_3$.

Table 2
Calculated elastic constants (C_{11}, C_{12}, and C_{44}), bulk modulus (B), tetragonal shear modulus ($G' = (C_{11} - C_{12})/2$), shear modulus (G), Young's modulus (E), B/G ratio, Cauchy pressure ($C_{12} - C_{44}$), Poisson's ratio (σ) and Lame's parameters (μ, λ) of $Sr_{1-x}La_xMoO_3$ (x = 0.0, 0.05, 0.1, 0.15, and 0.2) for MRIM.

Properties	0.0	0.05	0.1	0.15	0.2
C_{11} (GPa)	299.92	260.80	258.27	257.28	256.27
C_{12} (GPa)	83.71	72.87	72.98	73.12	73.27
C_{44} (GPa)	71.08	60.26	60.41	60.56	60.71
B (GPa)	155.78 145.77[a]	135.51	134.74	134.51	134.27
G' (GPa)	108.10	93.96	92.64	92.07	91.50
G (GPa)	84.12 69.50[a]	72.04	71.74	71.66	71.58
E (GPa)	213.88 180[a]	183.60	182.78	182.57	182.36
B/G	1.85	1.88	1.87	1.87	1.875
$C_{12} - C_{44}$ (GPa)	12.64	12.61	12.57	12.56	12.56
β (GPa^{-1})	0.00642 0.00686[a]	0.00737	0.00742	0.00743	0.00745
σ	0.271	0.274	0.273	0.273	0.273
μ	84.12	72.04	71.74	71.66	71.58
λ	99.70	87.48	86.91	86.73	86.54

[a] [37].

3.2. Elastic properties

The elastic properties, such as elastic constants (C_{11}, C_{12} and C_{44}), bulk modulus (B), tetragonal shear modulus (G'), shear modulus (G), Young's modulus (E), B/G ratio, Cauchy pressure ($C_{12} - C_{44}$), Poisson's ratio (σ), compressibility (β) and Lame's parameters (μ, λ) have been calculated using their expressions from Eqs. (4)–(13) and their values are listed in Table 2, together with reported experimental data (B, G, and E) reported by Yamanaka et al. [39]. To the best of our knowledge, there are no experimental and other theoretical results on the elastic constants for comparison of our results. Hence, our work is the first attempt in this direction.

Since C_{11}, C_{12} and C_{44} comprise the complete set of elastic constants for a cubic system, therefore, the bulk modulus (B), tetragonal shear modulus (G'), shear modulus (G), Young's modulus (E), compressibility (β) and Poisson's ratio (σ) can be derived from them.

All C_{ij} constants for $Sr_{1-x}La_xMoO_3$ compounds are positive and satisfy the generalized criteria [41] for mechanically stable crystals: $(C_{11} - C_{12}) > 0$, $(C_{11} + 2C_{12}) > 0$ and $C_{44} > 0$. Such compounds are characterized by positive values of the bulk modulus, shear modulus and tetragonal shear modulus.

The bulk modulus of these crystals decreases from concentration x = 0.0 to x = 0.2, i.e., in reversible sequence to lattice parameter. This is in agreement with the well-known relationship [42] between B and the lattice constants (cell volume V_o, as $B \sim {V_o}^{-1}$). This simple trend, when a larger lattice constant leads to a smaller bulk modulus, has been demonstrated also for various perovskite like materials [43]. The compressibility ($\beta = 1/B$) increases (from x = 0.2 to x = 0.0) as the value of the lattice parameter decreases. It was found for $Sr_{1-x}La_xMoO_3$: $B > G' > G$; this implies that the parameters limiting the mechanical stability of these materials are the shear modulus (G). The bulk modulus, shear modulus, Young's modulus and compressibility of $SrMoO_3$ computed from the elastic constants are in good agreement with experimental data [39].

The bulk modulus for $Sr_{1-x}La_xMoO_3$ slightly decreases with concentration in going from x = 0.0 to x = 0.2. Since a strong correlation exists between the bulk modulus and hardness of materials [44], the higher hardness should be for the pure $SrMoO_3$. This inference agrees with the behaviour of the shear modulus G (see Table 2). Indeed, the hardness of a material is defined as its resistance to another material penetrating to its surface, and this resistance is determined by the mobility of dislocations. Thus, one of the

Table 3
Calculated longitudinal, shear and average wave velocity (υ_l, υ_s and υ_m, respectively) and the Debye temperature (θ_D, θ_{D1}) of $Sr_{1-x}La_xMoO_3$ (x = 0.0, 0.05, 0.1, 0.15, and 0.2) for MRIM.

Properties	0.0	0.05	0.1	0.15	0.2
υ_s (ms^{-1})	3718	3424	3403	3383	3364
υ_l (ms^{-1})	6636	6139	6098	6062	6026
υ_m (ms^{-1})	4138	3813	3788	3767	3745
Θ_D (K)	297.74	274.19	272.22	270.63	269.06
Θ_{D1} (K)	460.81	427.17	424.54	421.91	419.53
	386.4[a], 510[b]	246.50[c]	221.00[c]	220.10[c]	198.10[c]

[a] [12].
[b] [37].
[c] [13].

Table 4
Calculated cohesive energy (ϕ), molecular force constant (f), Restrahalen frequency (υ_0) Gruneisen parameter (γ), thermal expansion coefficient (α), specific heat at constant volume (C_v) and specific heat at constant pressure (C_p) of $Sr_{1-x}La_xMoO_3$ (x = 0.0, 0.05, 0.1, 0.15, and 0.2) for MRIM.

Properties	0.0	0.05	0.1	0.15	0.2
ϕ (eV)	−163.75	−163.48	−163.35	−163.34	−163.32
f(10^{12} dynes/cm^2)	32.78	28.58	28.64	28.70	28.75
υ_0 (THz)	6.19	5.71	5.66	5.63	5.60
υ_1 (THz)	9.59	8.89	8.83	8.78	8.73
C_v (J/mol K)	110.07	111.83	111.96	112.09	112.22
C_p (J/mol K)	113.93	116.56	116.75	116.94	117.16
	107.79[b]	103.5[c]	108.9[c]	111.10[c]	115.9[c]
γ	2.65	2.69	2.70	2.71	2.73
α (10^{-5} K^{-1})	5.26	6.14	6.18	6.21	6.26
	7.98[a]				

[a] [37].
[b] [15].
[c] [13].

determining factors of hardness is the response of interatomic bonds to shear strain [45]. In our case, the shear modulus (G) is slightly lowered in the sequence from concentration x = 0.0 to x = 0.2, i.e., a higher bond-restoring energy under elastic shear strain should be for pure $SrMoO_3$, whereas $Sr_{0.8}La_{0.2}MoO_3$ will remain as a material with the lower hardness. Frantsevich [46] suggested to distinguish brittleness and ductility by Poisson's ratio. According to him [46], the critical value of Poisson's ratio of a material is 1/3. For brittle materials, the Poisson ratio is less than 1/3, and values larger than 1/3 can be regarded as ductile materials. The Poisson ratio in the present work is less than the critical value, i.e., 1/3. Therefore, $Sr_{1-x}La_xMoO_3$ can be considered as brittle materials.

On the other hand, Pugh [47] has proposed a simple relationship, empirically linking the plastic properties of materials with their elastic moduli. The shear modulus (G) represents the resistance to plastic deformation, while the bulk modulus (B) represents the resistance to fracture. A high B/G ratio may then be associated with ductility whereas a low value would correspond to a more brittle nature. The critical value which separates ductile and brittle materials is around 1.75, i.e., if $B/G > 1.75$ the material behaves in a ductile manner; otherwise the material behaves as a brittle. In case of these materials, the value of $B/G > 1.75$ (see Table 2), and they may therefore be classified as a ductile material.

Pettifor [48] has suggested that the angular character of atomic bonding in metals and compounds, which also relates to the brittle or ductile characteristics, could be described by the Cauchy pressure ($C_{12} - C_{44}$). For metallic bonding, the Cauchy pressure is typically positive. On the other hand, for directional bonding with angular character, the Cauchy pressure is negative, with larger negative pressure representing a more directional character. These correlations have been verified for ductile materials such as Ni and Al that have a typical metallic bonding, as well as for brittle semiconductors such as Si with directional bonding [48]. Based on the calculated (see Table 2), we conclude that these materials quite distinctly belong to the class of metallically bonding materials, i.e., they are ductile in behaviour. With the above discussion, we can conclude that $Sr_{1-x}La_xMoO_3$ (x = 0.0, 0.05, 0.1, 0.15, and 0.2) are ductile in nature.

The bulk and shear modulus are used to compute the longitudinal, shear and average wave velocities (υ_l, υ_s and υ_m, respectively) and are reported in Table 3.

3.3. Thermodynamic properties

The thermodynamic properties, such as cohesive energy (ϕ), molecular force constant (f), Debye temperature (θ_D, θ_{D1}), Restrahalen frequency (υ_0, υ_1), Gruneisen parameter (γ) and thermal expansion coefficient (α) of $Sr_{1-x}La_xMoO_3$ compounds have been calculated using the Eqs. (1), (17)–(25) and their values are listed in Tables 3 and 4 along with the experimental data [13,14,39].

The cohesive energy is the measure of strength of the force binding the atoms together in solids. This fact is exhibited from our cohesive energy results which follow the similar trend of variation with T, as is revealed by the bulk modulus that represents the resistance to volume change [49].

From Table 4 it is evident that the cohesive energy decreases from −163.75 eV for $SrMoO_3$ to −163.32 eV for $Sr_{0.8}La_{0.2}MoO_3$, calculated from the present interionic potential with La substitution. This is expected to be so due to the decrease in interionic separation. The cohesive energy shows the same trend of variation as exhibited by the bulk modulus. Although the values of the cohesive energy for different concentrations do not show much difference in their values, but the negative values of cohesive energy show that the stability of these molybdates is intact. However, their experimental values are not available yet in literature for comparison.

The concept of the Debye temperature has played an important role in the field of thermophysical properties of materials ever since its introduction. It is basically a measure of the vibrational response of the material and, therefore, intimately connected with properties like the specific heat, thermal expansion, and vibrational entropy [50]. The Debye temperature is not a strictly determined parameter; various estimates may be obtained through well-established empirical or semi-empirical formulae, relating Debye temperature with various macroscopic properties [51].

Debye temperatures (θ_D and θ_{D1}) can thus be derived from the average sound velocity υ_m and Restrahalen frequency (υ_1) (calculated from the molecular force constant (f)), respectively. These values are listed in Table 3 with the experimental data [13,14,39] for the comparison. The decrease in the bulk modulus on the other hand can result in the smaller Debye temperature in $Sr_{1-x}La_xMoO_3$. That is, as the bulk modulus decreases, a phonon hardening takes place and Debye temperature will decrease. The higher bulk modulus in $SrMoO_3$ results in the higher Debye temperature.

The decrease in molecular force constant with La doping (see Table 4) indicates decrease in the strength (or cohesive energy) of the crystal. The Restrahalen frequency is directly proportional to the molecular force constant and varies with the concentration accordingly. It is also seen from Table 4 that Restrahalen frequency and Gruneisen parameter are decreasing with the La doping. This trend of variations seems to be systematic as per the expectation. Here, it is noteworthy that the Gruneisen parameters for $Sr_{1-x}La_xMoO_3$ lie in between 2 and 3, as found in perovskites [52]. The thermal expansion coefficient $\alpha = 5.26 \times 10^{-5}$ K^{-1} of $SrMoO_3$ is in good agreement with the other theoretical data [39].

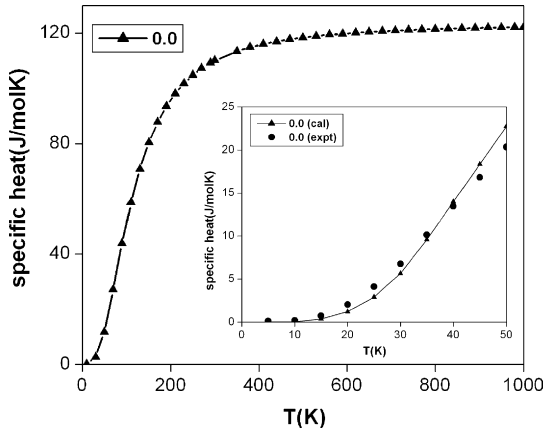

Fig. 1. Temperature dependence of specific heat of $SrMoO_3$ in the temperature range $10\,K \le T \le 1000\,K$. Inset shows the variation of the specific heat at $10\,K \le T \le 300\,K$ temperatures. The symbols (-▲-) and (●) represent the present calculated and experimental [15] results, respectively.

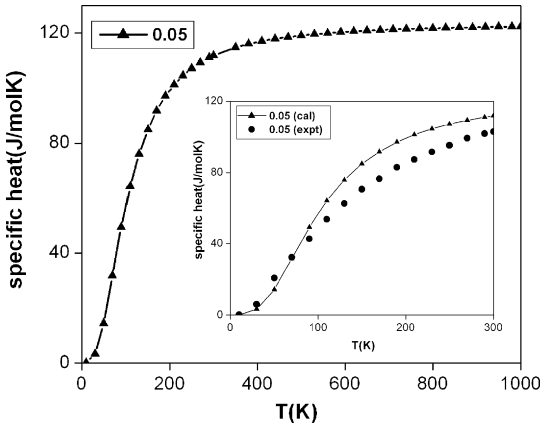

Fig. 2. The variations of the specific heat of $Sr_{0.95}La_{0.05}MoO_3$ in the wide temperature range, i.e., $10\,K \le T \le 1000\,K$. The symbols (-▲-) and (●) represent the present calculated and experimental [13] results, respectively.

3.4. Specific heats (C_v and C_p)

The investigation of the specific heat of crystals is an old topic of the condensed matter physics with which illustrious names are associated [53–55]. The knowledge of the specific heat of a substance not only provides essential insight into its vibrational properties but is mandatory for many applications. Two famous limiting cases had been correctly predicted by the standard elastic continuum theory [55].

The values of specific heats (C_v and C_p) computed for $Sr_{1-x}La_xMoO_3$ at 300 K have been presented in Table 4. The calculated specific heats, at ambient condition, for $Sr_{1-x}La_xMoO_3$ ($x = 0.05$, 0.1, 0.15, and 0.2) are consistent with the experimental values [14,4,39]. The discrepancy between the experimental [14,4,39] and our calculated values of $Sr_{1-x}La_xMoO_3$ is because of the difference in their Debye temperatures. The variation in Mo–O distance by the substitution of Sr by La decreases Debye temperature and hence there is a consistent increase in the specific heat values corresponding to the substitution (see Table 4). Hence, the concentration (x) dependence of Debye temperature in $Sr_{1-x}La_xMoO_3$ ($x = 0.0$, 0.05, 0.1, 0.15, and 0.2) suggests that the increased La doping drives the system effectively far from the strong electron–phonon coupling regime.

We have applied our MRIM to compute the specific heat of $Sr_{1-x}La_xMoO_3$ ($x = 0.0$, 0.05, 0.1, 0.15, and 0.2) compounds in the temperature range $10\,K \le T \le 1000\,K$. The temperature variations of the specific heats of these compounds are depicted in Figs. 1–5, respectively. The variation trend (as shown in the inset of Figs. 1–5) of the present specific heat curves for $Sr_{1-x}La_xMoO_3$ ($x = 0.0$, 0.05, 0.1, 0.15, and 0.2) are, in good agreement with the corresponding experimental results [14,4,39] available in the range, 10–300 K [14,4]. The agreement between our theoretical and available experimental [14,4] data is reasonably good at lower temperatures (10–150 K) as our MRIM model is subject to the harmonic approximation. However, the remarkable deviations appearing at higher temperatures ($150\,K \le T \le 300\,K$) are due to the anharmonic effects [56,57], whose contributions are very well demonstrated by Jindal and Kalus [56] and Jindal et al. [57] for other materials. Thus, we can interpret our results on specific heats from $10\,K \le T \le 1000\,K$ as follows:

At high temperatures, the specific heat tends to the Petit and Dulong limit [58]. At low temperatures, specific heat is proportional to T^3 [55]. At intermediate temperatures, however, the temperature dependence of specific heat is governed by the details of vibrations of the atoms and for a long time could only be determined from experiments. The sharp increase, around ~300 K, is due to the anharmonic effects [56,57]. However, at higher temperatures, the anharmonic effect on specific heat is suppressed and it is very close to the Dulong–Pettit limit [58], which is common to all solids at high temperatures. The specific heats in these materials vary almost lin-

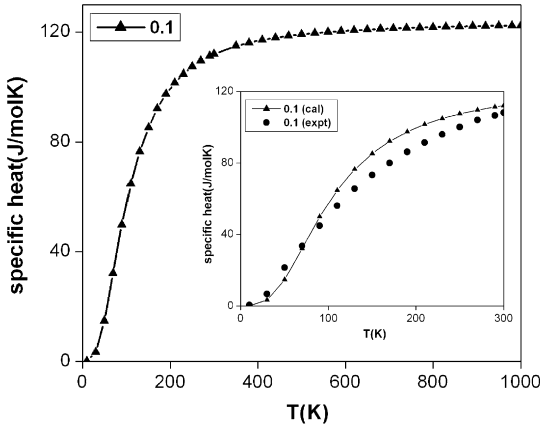

Fig. 3. The variations of the specific heat of $Sr_{0.9}La_{0.1}MoO_3$ in the wide temperature range, i.e., $10\,K \le T \le 1000\,K$. The symbols (-▲-) and (●) represent the present calculated and experimental [13] results, respectively.

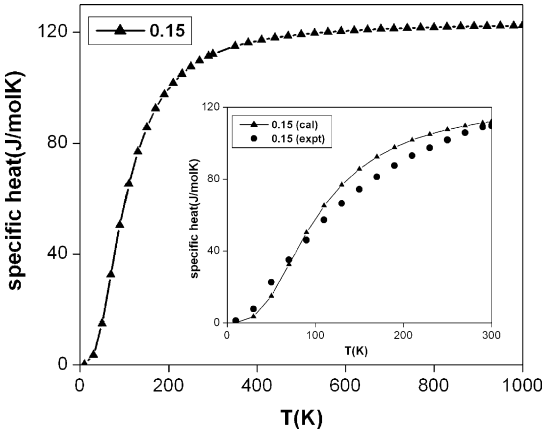

Fig. 4. The variations of the specific heat of $Sr_{0.85}La_{0.15}MoO_3$ in the wide temperature range, i.e., $10\,K \le T \le 1000\,K$. The symbols (-▲-) and (●) represent the present calculated and experimental [13] results, respectively.

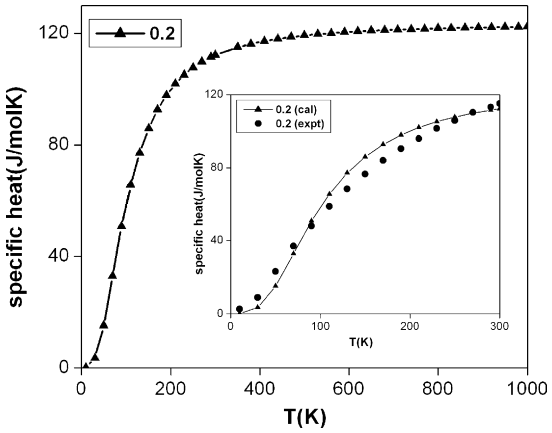

Fig. 5. The variations of the specific heat of $Sr_{0.8}La_{0.2}MoO_3$ in the wide temperature range, i.e., $10\,K \leq T \leq 1000\,K$. The symbols (–▲–) and (●) represent the present calculated and experimental [13] results, respectively.

early between 0 and 200 K and later on vary along curvature from 200 to 500 K and finally become almost constant beyond 600 K.

We could not compare some of our results at higher temperatures, due non-availability of the experimental data. The present work probably, the first report on them. At present they are only of academic interest but will certainly work as a guide to the experimental workers in the future.

4. Conclusions

The varied exposition of the elastic and thermodynamic properties of pure and doped perovskite system ($SrMoO_3$) attained by us is remarkable in view of the inherent simplicity of the modified rigid ion model. This indicates the strength and usefulness of the MRIM as having the potential to explain a variety of elastic properties (such as C_{11}, C_{12}, C_{44}, B, G', G, E, σ, β, μ, λ, υ_l, υ_s and υ_m) and thermodynamical properties (such as ϕ, f, θ_D, θ_{D1}, υ_0, υ_1, γ, α_v, C_v and C_p) of the pure and doped $SrMoO_3$ materials. However, the efforts that have been devoted by many experimental workers to study the elastic and thermodynamic properties, to the best of our knowledge, only a few theoretical studies have been performed on the temperature- and composition-dependent properties of the perovskite molybdate materials. On the basis of the overall descriptions, it may be concluded that our modified rigid ion model has reproduced elastic and thermodynamic properties that correspond well to the experimental data. Here, some of the results could not be compared due to lack of experimental data on them. These results are at present of academic interest but they will certainly serve as a guide to the experimental workers in future.

Acknowledgement

The authors are grateful to The University Grants Commission (UGC), New Delhi for providing the financial support for this work.

References

[1] J.G. Bednorz, K.A. Muller, Z. Phys. B64 (1986) 189.
[2] S. Jin, T.H. Tiefel, M. McCormack, R.A. Fastnacht, R. Ramesh, L.H. Chen, Science 264 (1994) 413.
[3] Y.S. Lee, J.S. Lee, T.W. Noh, D.Y. Byun, K.S. Yoo, K. Yamaura, E.T. Muromachi, Phys. Rev. B 67 (2003) 113101.
[4] R. Agarwal, Z. Singh, V. Venugopal, J. Alloys Compd. 282 (1999) 231.
[5] S.I. Ikeda, N. Shirakawa, Physica C 341 (2000) 785.
[6] A. Radetinac, K.S. Takahashi, L. Alff, M. Kawasaki, Y. Tokura, Appl. Phys. Express 3 (2010) 073003.
[7] P. Kostic, Y. Okada, N.C. Collins, Z. Schlesinger, J.W. Reiner, L. Klein, A. Kapitulnik, T.H. Geballe, M.R. Beasley, Phys. Rev. Lett. 81 (1998) 2498.
[8] I. Nagai, N. Shirakawa, S.I. Ikeda, R. Iwasaki, H. Nishimura, M. Kosaka, Appl. Phys. Lett. 87 (2005) 024105.
[9] J.B. Goodenough, J. Appl. Phys. 37 (1966) 1415.
[10] J.B. Goodenough, J.M. Longo, Landolt-Bonstein Zahlenwerte und Funktionen, New Series BdIII/4a, (1970) 255.
[11] S.B. Zhang, Y.P. Sun, B.C. Zhao, X. Luo, C.Y. Hao, X.B. Zhu, W.H. Song, J. Appl. Phys. 102 (2007) 103903.
[12] B.C. Zhao, Y.P. Sun, S.B. Zhang, X.B. Zhu, W.H. Song, Solid State Commun. 138 (2006) 219.
[13] B.C. Zhao, Y.P. Sun, S.B. Zhang, W.H. Song, J.M. Dai, J. Appl. Phys. 102 (2007) 113903.
[14] S.B. Zhang, Y.P. Sun, B.C. Zhao, X.B. Zhu, W.H. Song, Phys. Status Solidi (b) 243 (2006) 1331.
[15] S.B. Zhang, Y.P. Sun, B.C. Zhao, X.B. Zhu, W.H. Song, Solid State Commun. 138 (2006) 123.
[16] S. Yamanaka, T. Hamaguchi, T. Oyama, T. Matsuda, S. Kobayashi, K. Kurosaki, J. Alloys Compd. 359 (2003) 1.
[17] S. Yamanaka, M. Fujikane, T. Hamaguchi, H. Muta, T. Oyama, T. Matsuda, S. Kobayashi, K. Kurosaki, J. Alloys Compd. 359 (2003) 109.
[18] K. Kurosaki, T. Oyama, H. Muta, M. Uno, S. Yamanaka, J. Alloys Compd. 372 (2004) 65.
[19] S. Yamanaka, T. Maekawa, H. Muta, T. Matsuda, S. Kobayashi, K. Kurosaki, J. Solid State Chem. 177 (2004) 3484.
[20] M. Kawachi, M. Abe, S. Nomura, J. Phys. Soc. Jpn. 34 (1973) 372.
[21] R.B. Macquart, B.J. Kennedy, M. Avdeev, J. Solid State Chem. 183 (2010) 250.
[22] D. Logvinovicha, R. Aguiarb, R. Roberta, M. Trottmanna, S.G. Ebbinghausb, A. Rellerb, A. Weidenkaffa, J. Solid State Chem. 180 (2007) 2649.
[23] N. Kaur, R. Mohan, N.K. Gaur, R.K. Singh, Ind. J. Pure Appl. Phys. 46 (2007) 447.
[24] A. Srivastava, N.K. Gaur, N. Kaur, R.K. Singh, J. Mag. Mag. Mater. 320 (2008) 2598.
[25] M.N. Rao, N. Kaur, S.L. Chaplot, N.K. Gaur, R.K. Singh, J. Phys.: Condens. Matter 21 (2009) 355402.
[26] R. Choithrani, N.K. Gaur, J. Mag. Mag. Mater. 320 (2008) 612.
[27] R. Choithrani, N.K. Gaur, A. Srivastava, Solid State Commun. 145 (2008) 308.
[28] N. Kaur, N.K. Gaur, R.K. Singh, Mod. Phys. Lett. B 21 (2007) 885.
[29] N. Kaur, R. Mohan, N.K. Gaur, R.K. Singh, Physica C 451 (2007) 24;
N. Kaur, R. Mohan, N.K. Gaur, R.K. Singh, J. Phys. Chem. Solids 68 (2007) 2247.
[30] D.W. Hafemiester, W.H. Flygare, J. Chem. Phys. 43 (1965) 795.
[31] M.P. Tosi, F.G. Fumi, J. Phys. Chem. Solids 23 (1965) 359;
M.P. Tosi, Solid State Phys. 2 (1964) 1.
[32] J.C. Slater, K.G. Kirkwood, Phys. Rev. 37 (1931) 682.
[33] R.K. Singh, Phys. Rep. 85 (1982) 259.
[34] D. Varshney, N. Kaurav, R. Kinge, R.K. Singh, J. Phys.:Condens. Matter 19 (2007) 236204;
D. Varshney, N. Kaurav, R. Kinge, R.K. Singh, J. Phys.:Condens. Matter 19 (2007) 346212.
[35] L. Pauling, Z. Kristallogr. 67 (1928) 377;
L. Pauling, J. A. C. S. 50 (1928) 1036;
Pauling, 1945 L. Pauling, The Nature of the Chemical Bond, Cornell University Press, Ithaca, 1945.
[36] N. Kaur, R. Mohan, N.K. Gaur, R.K. Singh, J. Alloys Compd. 491 (2010) 284.
[37] E. Schreiber, O.L. Anderson, N Soga, Elastic Constants and their Measurements, McGraw-Hill, New York, 1973.
[38] O.L. Anderson, J. Phys. Chem. Solids 24 (1963) 909.
[39] S. Yamanaka, K. Kurosaki, T. Maekawa, T. Matsuda, S. Kobayashi, M. Uno, J. Nucl. Mater. 344 (2005) 61.
[40] K.B. Modi, M.C. Chhantbar, P.U. Sharma, H.H. Joshi, J. Mater. Sci. 40 (2005) 1247.
[41] G.V. Sin'ko, N.A. Smirnow, J. Phys.: Condens. Matter 14 (2002) 6989;
J. Wang, S. Yip, S.R. Phillpot, D. Wolf, Phys. Rev. Lett. 71 (1993) 4182.
[42] M.L. Cohen, Phys. Rev. B 32 (1985) 7988.
[43] R.D. King-Smith, D. Vanderbilt, Phys. Rev. B 49 (1994) 5828.
[44] J. Haines, J.M. Leger, G. Bocquillon, Annu. Rev. Mater. Res. 31 (2001) 1.
[45] S.H. Jhi, J. Ihm, S.G. Louie, M.L. Cohen, Nature (Lond.) 399 (1999) 132.
[46] I.N. Frantsevich, F.F. Voronov, S.A. Bokuta, in: I.N. Frantsevich (Ed.), Elastic Constants and Elastic Moduli of Metals and Insulators Handbook, Naukova Dumka, Kiev, 1983, p. 60.
[47] S.F. Pugh, Philos. Mag. 45 (1954) 823.
[48] D. Pettifor, Mater. Sci. Technol. 8 (1992) 345.
[49] M.N. Iliev, M.V. Abrashev, J. Laverdiere, S. Jandl, M.M. Gospodinov, Y.Q. Wang, Y.Y. Sun, Phys. Rev. B 73 (2006) 064302.
[50] G. Grimvall, Thermophysical Properties of Materials, North Holland, Amsterdam, 1956.
[51] H.M. Leadbetter, in: R.P. Reep, A.F. Clark (Eds.), Elastic Properties of Materials at Low Temperatures, ASM Metal Park, Ohio, 1983.
[52] P. Dai, Z. Jiandi, H.A. Mook, S.H. Lion, P.A. Dowben, E.W. Plummer, Phys. Rev. B 54 (1996) R3694.
[53] A. Einstein, Ann. Phys. 22 (1907) 180.
[54] W. Nernst, A.F. Lindemann, Z. Elektrochem, Angew. Phys. Chem. 17 (1977) 817.
[55] P. Debye, Ann. Phys. 39 (1912) 789.
[56] V.K. Jindal, J. Kalus, J. Phys. C: Solid State Phys. 16 (1983) 3061.
[57] V.K. Jindal, R. Righini, S. Califano, Phys. Rev. B 38 (1988) 4259.
[58] A.T. Petit, P.L. Dulong, Ann. Chim. Phys. 10 (1819) 395.